Investigation of image properties in the SIBERIA project

Jiong Jiong Yu and Shaun Quegan
SCEOS
25/10/99

1. Introduction

The properties of images acquired by different SAR systems may vary. Important differences arise due to different configurations of wavelength, polarization and resolution employed in the systems. More subtle differences come from the data processing, especially the strategy for combining looks and resampling. These can have a big impact on the data handling, error analysis and image operations such as filtering. Appropriate treatment of the data requires that one should have the correct knowledge of the image being dealt with. In this report, three important aspects of image properties are investigated, namely spatial correlation, equivalent number of looks (ENL) and texture. The investigation is carried out using the Bratsk data set, including the ERS intensity image acquired on 23/9/97 (Figure 1(a)), the JERS intensity on 4/5/97 (Figure 1(b)), and the 80-pixel and 20-pixel coherence images (Figure 1(c) and (d)). Histograms are also shown underneath each image. The two intensity images are scaled to the same dynamic range, as are the two coherence images.

2. Measurements of image properties

2.1 Equivalent number of looks (ENL)

The equivalent number of looks (ENL), measures the number of *independent* intensity values averaged per pixel. ENL is related to the coefficient of variation (CV) by

$$ENL = \frac{1}{CV^2} = \frac{\langle I \rangle^2}{\mathrm{var}(I)} \tag{1}$$

where the mean and variance of intensity are denoted by $\langle I \rangle$ and var(I).

The intensity in an untextured L-look image is Gamma distributed with order parameter L.

$$P_I(I) = \frac{1}{\Gamma(L)} \left(\frac{L}{s} \right)^L I^{L-1} e^{-LI/s}$$

where $s = \langle I \rangle$ is the mean. The mean and variance in the gamma distribution are related by $\mathrm{var}(I) = \frac{\langle I \rangle^2}{L}$. Hence the theoretical ENL value for a multi-look Gamma distributed image is equal to the order parameter L. Note that, in practice, $\langle I \rangle$ is estimated by $\hat{I} = \frac{1}{M}\sum_{i=1}^{M} I_i$ and the unbiased estimate for var(I) is $V(I) = \frac{1}{M}\sum_{i=1}^{M}\left(I_i - \hat{I}\right)^2$, where M is the number of pixels inside the window. If the pixels are uncorrelated, the maximum likelihood estimator (MLE) of the mean is also given by spatial averaging, i.e. $\frac{1}{M}\sum_{i=1}^{M} I_i$. It needs to be stressed that spatial averaging is the MLE of the mean only if the pixels are uncorrelated. For a discussion on spatial correlation, see Section 2.2.

Three homogeneous areas were selected in the intensity ERS (Figure 1(a)) and JERS (Figure 1(b)) images. For each area, the values of mean and variance were measured, and the corresponding ENLs were calculated according to Equation (1) (Table 1).

Note that ENL can be noninteger due to correlation between looks. In order to find the closest ENL, Gamma distributions with orders between 11 – 15 have been overlaid on the histograms of the observations from the ERS data. It was found visually that the 12-look Gamma fits the measured values best (Figure 2(a)), although the discrepancies in the interval 0.1 - 0.2 are significant. Note that the values given in Table 1 suggest that, despite the reasonable fit for 12 looks, the true ENL for ERS is near 14 or 15. Observed values as high as those in the Table are very unlikely if ENL ~ 12. The regions are "too smooth" to have come from 12-look speckle. It is easy to reduce the measured numbers of looks; this will happen if the region is not homogeneous, but increased numbers of looks can only come from statistical fluctuation. The same experiment was repeated for the JERS data, with orders in the range 4 – 8. The results show good agreement between the 6-look Gamma distribution and data (Figure 2(b)). The Table suggests that the true ENL $\geq$ 6. Similar ENL values for the ERS and JERS data have been reported by Ursula M of DLR and Urs W of Gamma.

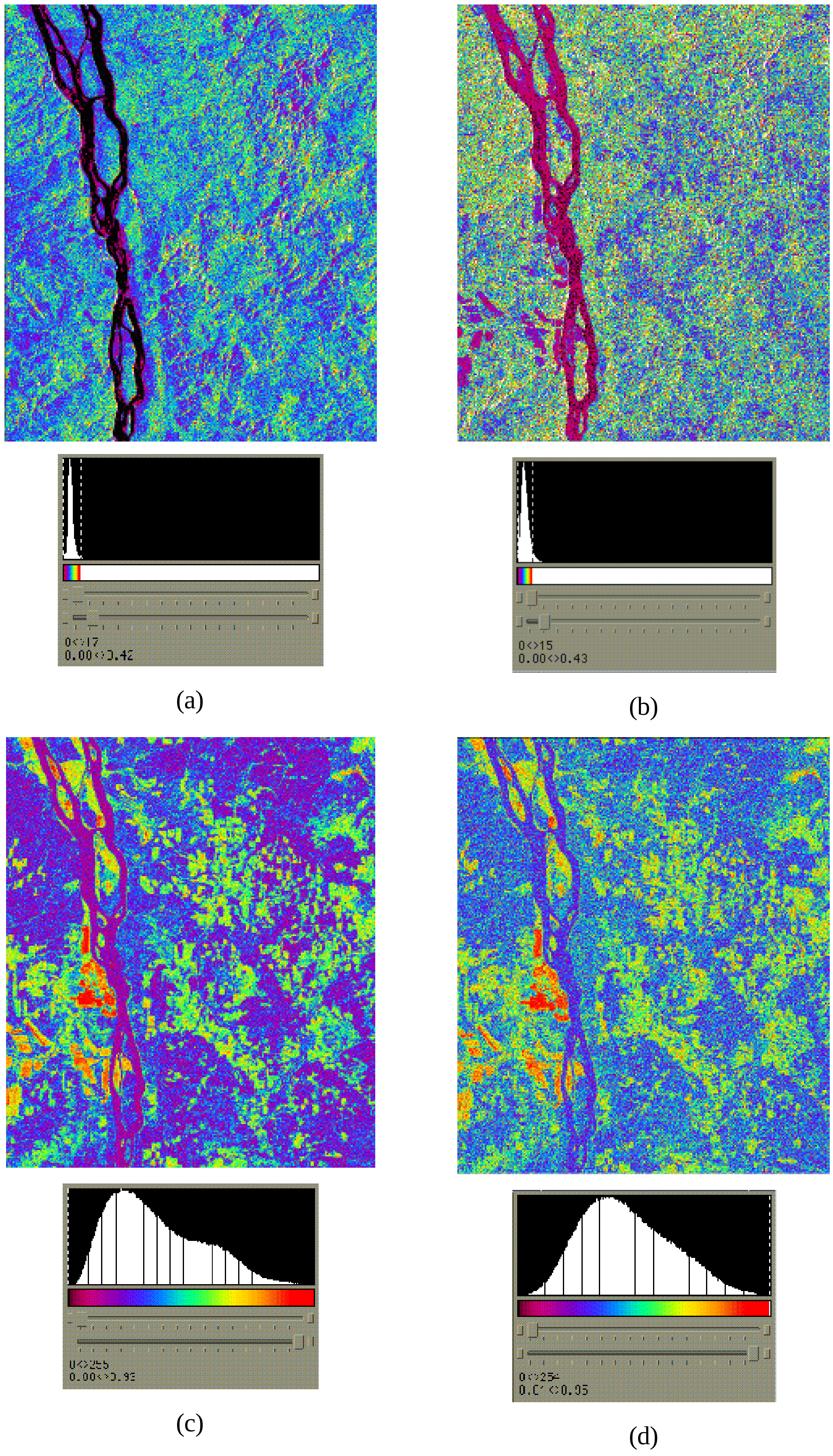

Figure 1-1 Bratsk images with corresponding histograms: (a) ERS-1 intensity on 23/9/97; (b) JERS-1 intensity on 4/5/97; (c) 80-pixel coherence and (d) 20-pixel coherence.

Data	sample	sample size (no. of pixels)	$\hat{I}$	$V(I)$	ENL
ERS	(a)	4080	0.1695	0.0018	15.74
	(b)	6229	0.1723	0.0022	13.63
	(c)	2285	0.1226	0.0012	13.06
JERS	(a)	4080	0.4799	0.0037	6.18
	(b)	6229	0.4304	0.0445	4.17
	(c)	2285	0.3592	0.0301	4.28

Table 1 Estimated mean, variance and ENL from visually homogeneous areas in Figure 1(a) and (b).

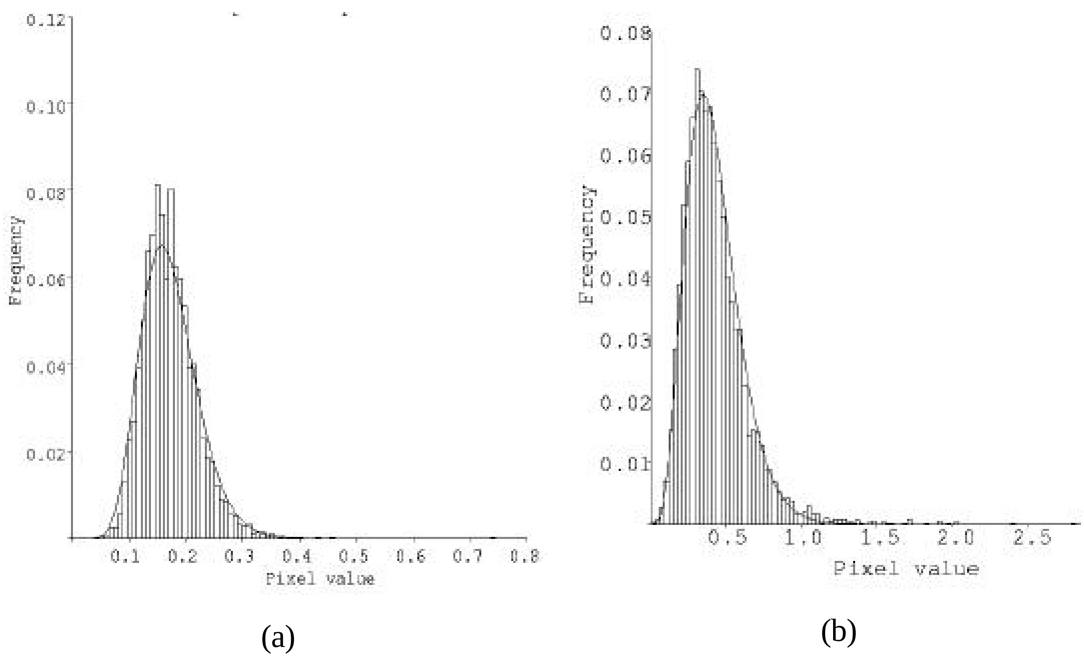

Figure 2 Histograms of measured values in (a) ERS data, superimposed on a 12-look gamma distribution; (b) JERS, superimposed on a 6-look gamma distribution.

2.2 Spatial correlation

Spatial correlation is an important aspect to take account of in image analysis. Many filters and analysis techniques assume uncorrelated data and the number of independent samples in a window is affected by this. In the following, the degree of correlation in the images displayed in Figure 1 is examined.

The correlation can be measured by use of the intensity autocorrelation. The range and azimuth intensity autocorrelation, r_r and r_a, are defined as

$$r_r(k) = \frac{\langle I_{i,j+k} I_{i,j} \rangle - \langle I \rangle^2}{\mathrm{var}(I)} \tag{2}$$

$$r_a(k) = \frac{\langle I_{i+k,j} I_{i,j} \rangle - \langle I \rangle^2}{\mathrm{var}(I)} \tag{3}$$

where k is the lag, i.e. the distance from the middle pixel in the area that is being examined, $I_{i,j}$ is the intensity at pixel (i, j), i.e. (azimuth, range), $\langle I \rangle$ is the mean of the intensity and var(I) is the variance.

The measured r_r and r_a from a homogeneous area (mature stand No. 5) in the images in Figure 1 are plotted as functions of lag in Figure 3. The important points are:

(a) From Figure 3(a), it can be seen that pixels in ERS data are significantly correlated, with r_r and r_a around 0.5 at lag~1; and r_r and r_a around 0.2 at lag~2;

(b) The degree of correlation is much less in JERS (Figure 3(b)) than in ERS; r_r and r_a are indistinguishable from noise (< 0.2 at all lags). So the pixels in JERS data can be considered as uncorrelated;

(c) In the 80-pixel coherence (Figure 3(c)), the only significant correlation is found at lag~1, where r_r and r_a are close to 0.5. From lag~2 and onwards, the correlation is mainly from noise;

(d) In the 20-pixel coherence (Figure 3(d)), r_r and r_a are around 0.2 when lag = 1. The correlation in both directions is insignificant at lags greater than 1.

In Section 2.1, it is mentioned that spatial averaging is the MLE of the mean intensity, based on the assumption that pixels are uncorrelated and independent of each other. From the above observations, it can be seen that $\frac{1}{M}\sum_{i=1}^{M} I_i$ can be treated as the MLE of the JERS mean intensity. For correlated ERS data, if complex data is available, then the MLE of the mean intensity of an M x N block of data is given by [Oliver & Quegan]

$$\hat{s} = \frac{1}{MN} tr\left(R_\mathrm{S}^{-1}\mathbf{S}\mathbf{S}^{\oplus}\right) = \frac{1}{MN}\mathbf{S}^{\oplus}R_\mathrm{S}^{-1}\mathbf{S}$$

where R_S is the correlation matrix of the N complex samples $\mathbf{S} = (S_1, \ldots S_{MN})$, $^{\oplus}$ denotes conjugate transpose, and tr denotes trace.

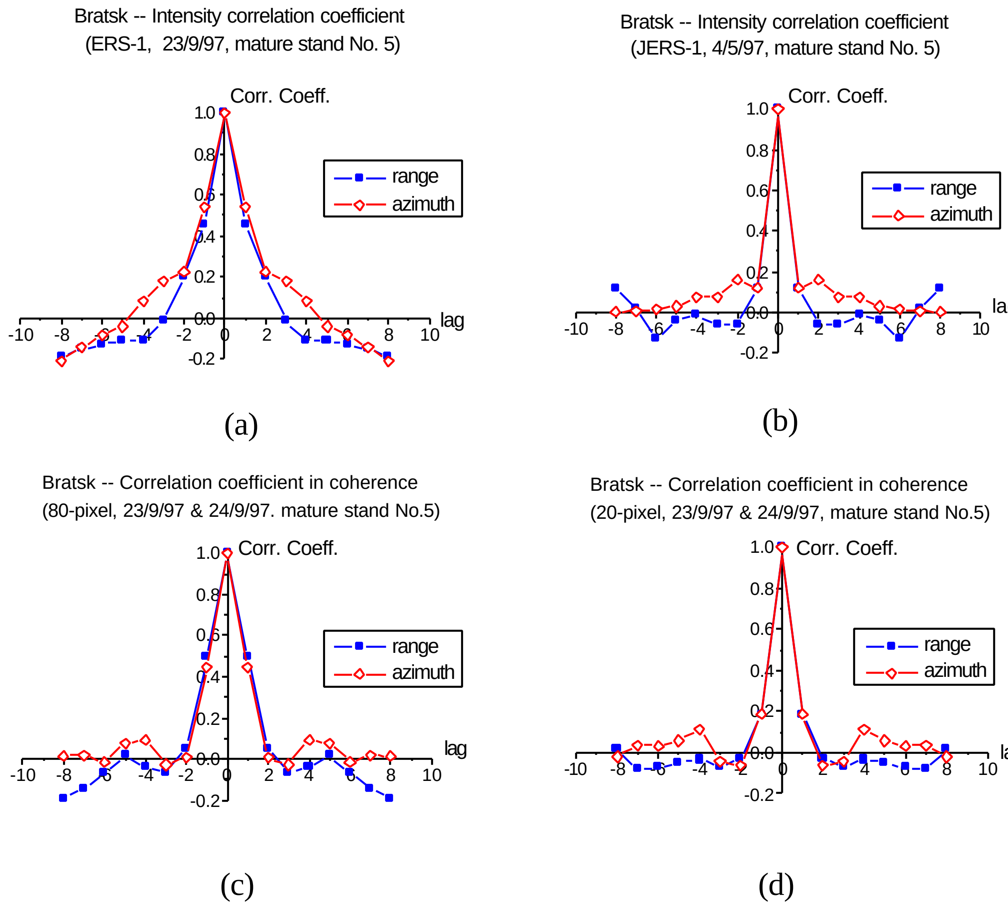

Figure 3 Intensity correlation coefficients calculated in the range and azimuth directions from a homogeneous area for: (a) ERS data and (b) JERS data with pixel spacing of 50m. Correlation coefficients in both directions for (c) 80-pixel coherence and (d) 20-pixel coherence.

2.3 Texture

In addition to the mean intensity, texture is another potential information source in SAR images, and different data models are used for textured and untextured images. Multi-look pure-speckle images are described by the Gamma model, whereas textured images are often characterized by the k-distribution.

Texture depends greatly on resolution. In spaceborne images, e.g. ERS-1/2, texture is expected to be averaged out, especially in vegetated areas. There are many approaches for quantitative measurements of texture. The two most commonly used are (1) the coefficient of variation, in which large values correspond to high texture, and (2) the normalized log measurement defined by [Oliver & Quegan]

$$T = \langle \ln I \rangle - \ln \langle I \rangle \qquad \textbf{(4)}$$

Equation (4) in fact approximates the order of the k-distribution. As this order parameter gets bigger, the data tends to be Gamma distributed, i.e. untextured. Hence high image texture is represented by low values of the normalized log.

Texture is measured for Figure 1(a) and (b) using the above two methods. The intensity coefficient of variation is displayed in Figure 4. In order to investigate the effect of window sizes on the texture estimation, results obtained using windows with sizes 5x5 and 11x11 pixels are shown side by side. Histograms are also shown for each image. The log measurements are displayed in Figure 5, using the same layout as in Figure 4. Adaptive estimation was also investigated, but the results are not much different to those in Figures 4 and 5.

Note that the texture measured by the CV is in fact the inverse of the square root of ENL (Equation 1). As JERS and ERS data have different numbers of looks (see Section 2.1), for comparison purposes, the images in Figure 4 have been thresholded with an upper boundary at 90% of the total number of pixels; and images in Figure 5 have a lower boundary at 10%. The following points should be noted:

(1) In all measurements, there is little evidence of texture. The structures observed in fact are features in the images:

    (a) In ERS measurements, Figures 4(a, b) and 5(a, b), high texture corresponds to the river and topography;

    (b) Due to the difference in incidence angles, reduced topographic effects but more features and lines are picked out in JERS (Figures 4(c, d) and 5(c, d)) than ERS. The overlay of Figure 4(d) with Figure 1 (c), displayed as Figure 7, shows that the features observed in the JERS texture do not correspond to stand information or land classes, for example young stands and clearcuts etc. They are more related to areas with relatively large coherence change in the surrounding areas. This causes the breakdown of the local box estimator.

(2) The intensity CV and normalized log measurement are “inverses” of each other, the high CV values associated with topography correspond to low values in the normalized log. Note that the log measurement is always less than zero. For easy comparison, the negative images of those in Figure 5 were produced with an upper boundary at 90% of the total number of pixels, shown as Figure 6. This reverses the histograms in Figure 5, and the colour schemes are more comparable with Figure 4. From Figures 4, 5 and 6, it can be seen that the texture information contained in the two measurements is very

similar;

(3) Not surprisingly, the texture images resulting from a 5x5 window have finer details than those from a 11x11 window, and the latter appear less noisy. The 11x11 window also enlarges the size of the bright points in the images. Depending on the application, both window sizes could be useful.

3. Conclusions

In this report, the image properties, ENL, spatial correlation and texture, have been investigated for the SIBERIA data, including ERS and JERS intensity images with pixel spacing of 50m, and ERS coherence images generated using 20-pixel and 80-pixel windows. The main conclusions are:

a. The ENLs are > 12 (probably around 14 - 15) for the ERS data and 6 for the JERS data;
b. The pixels in the JERS data are almost uncorrelated, with correlation coefficients less than 0.2 at all non-zero lags in both range and azimuth directions;
c. The ERS data has high correlation at lag 1 and lag 2. This implies that spatial averaging is not the MLE of the mean in the ERS image. However, this method is unbiased and is used for its simplicity and acceptable accuracy;
d. The correlation at lags > 1 in the 80-pixel and 20-pixel coherence images is not significant. Correlation is only significant at lag = 1 in 80-pixel coherence;
e. Two measures, namely the coefficient of variation and the normalized log, have been used for examining the texture information in both ERS and JERS data at window sizes of 5 x 5 and 11 x 11. The results show no evidence for texture in vegetated areas in either data set. The observed “texture” is feature-related, mainly arising from the river and topography;

The correlation in ERS data means that multilook averaging will result in the number of looks smaller than the theoretical value. The evidence above suggests that methods developed for the Gamma distribution are appropriate for both ERS and JERS data. Filtering methods based on the k-distribution, such as Gamma MAP, are not matched to the data properties.

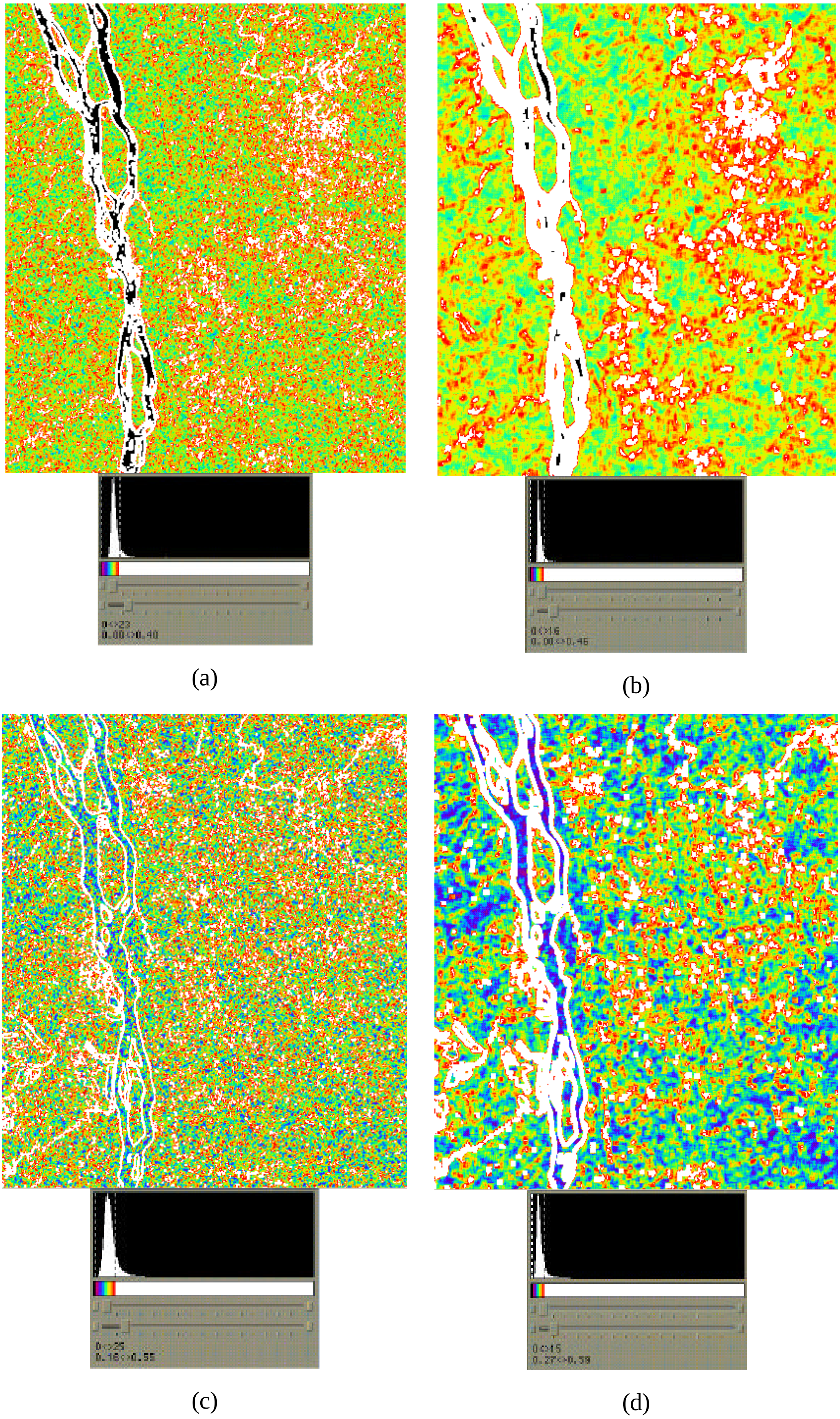

Figure 4 Intensity CV of (a) ERS and (c) JERS data, estimated using a 5x5 window; (b, d) are the same as (a, c), but using a 11x11 window.

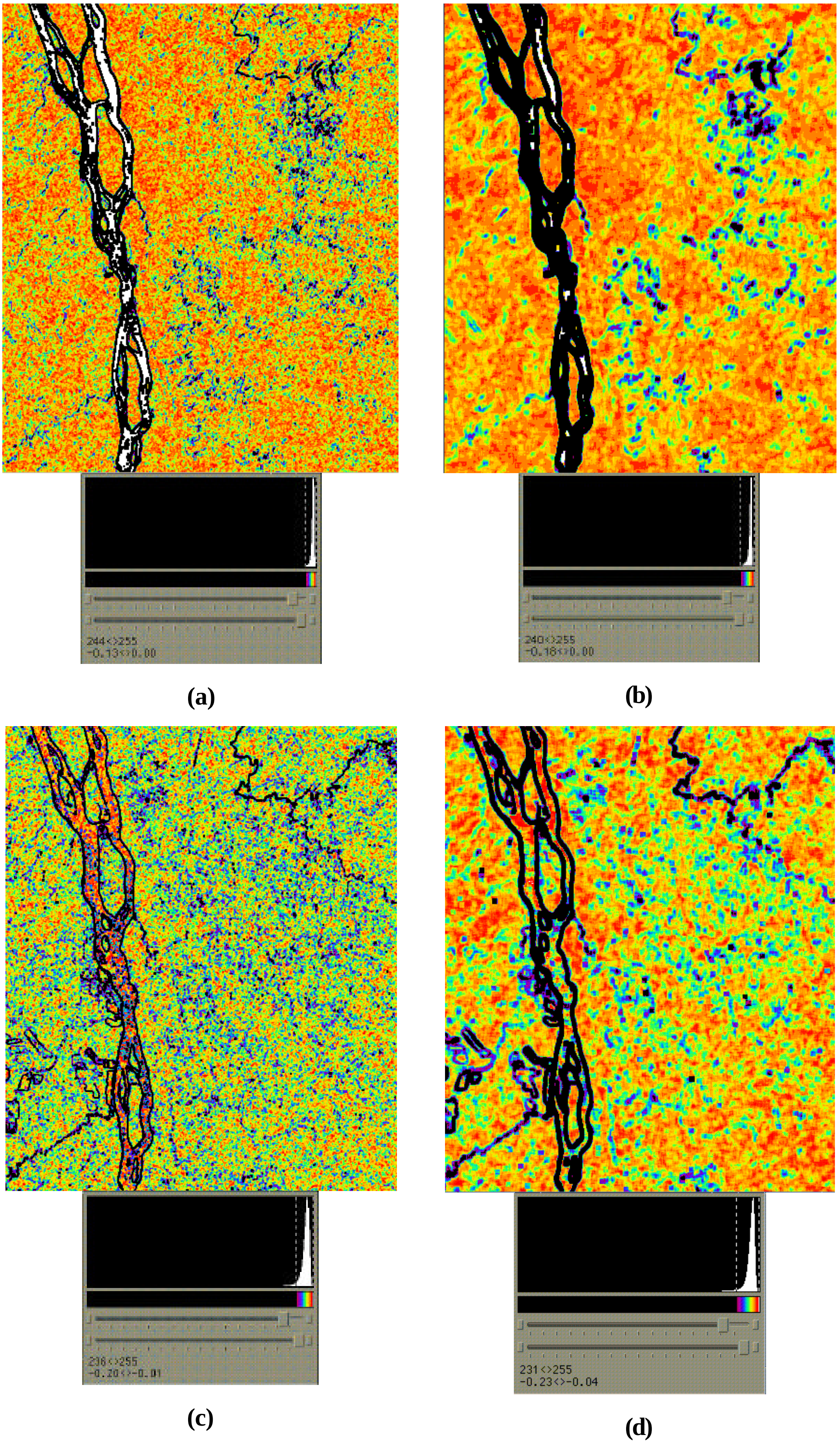

Figure 5 Normalized log measurement of (a) ERS and (c) JERS, estimated using a 5x5 window; (b, d) are the same as (a, c), but using a 11x11 window.

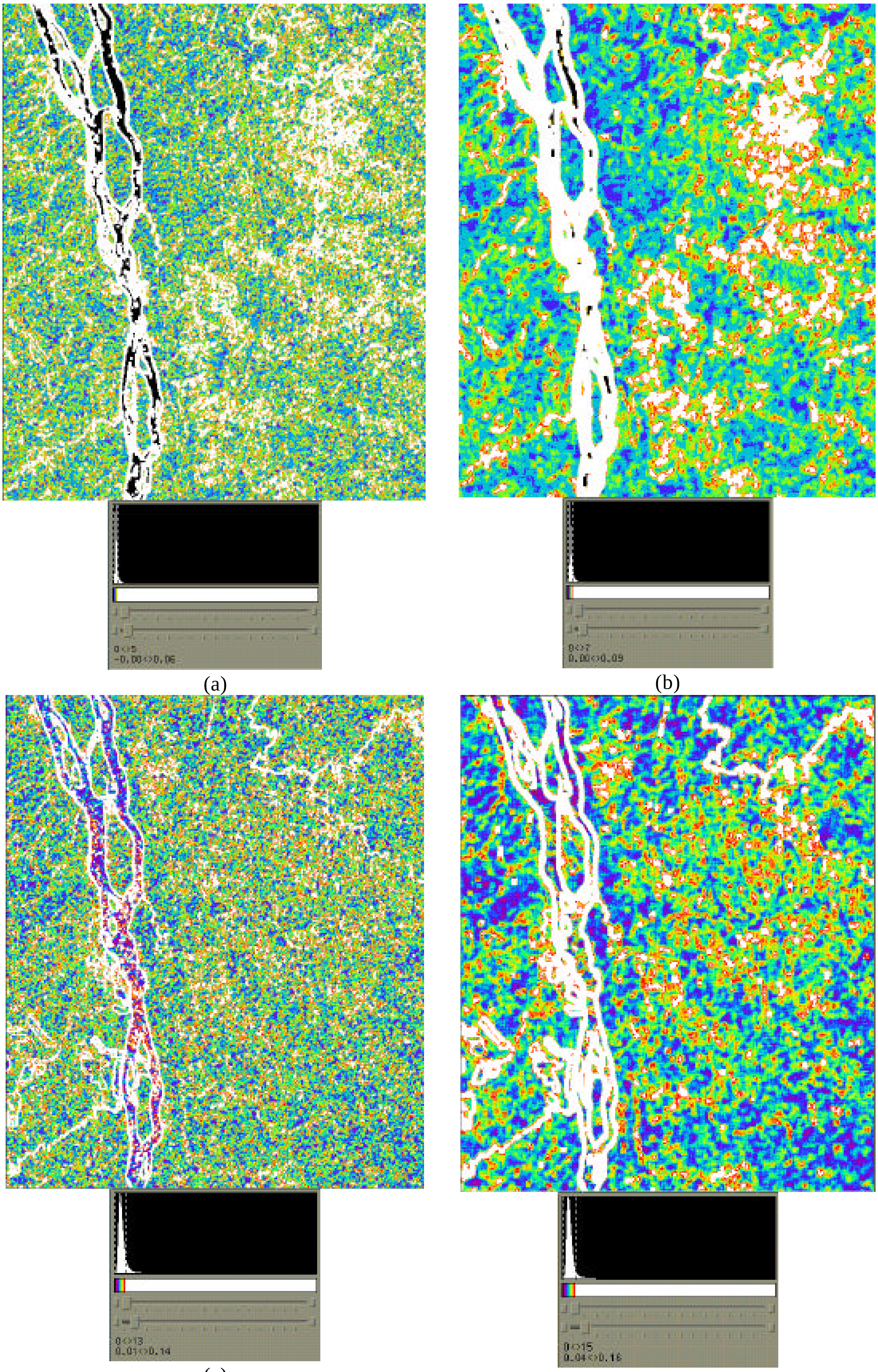

(a) (b)

(c)

Figure 6 Negative images of the normalized log measurements in Figure 5: (a) ERS and (c) JERS, estimated using a 5x5 window; (b, d) are the same as (a, c), but using a 11x11 window.

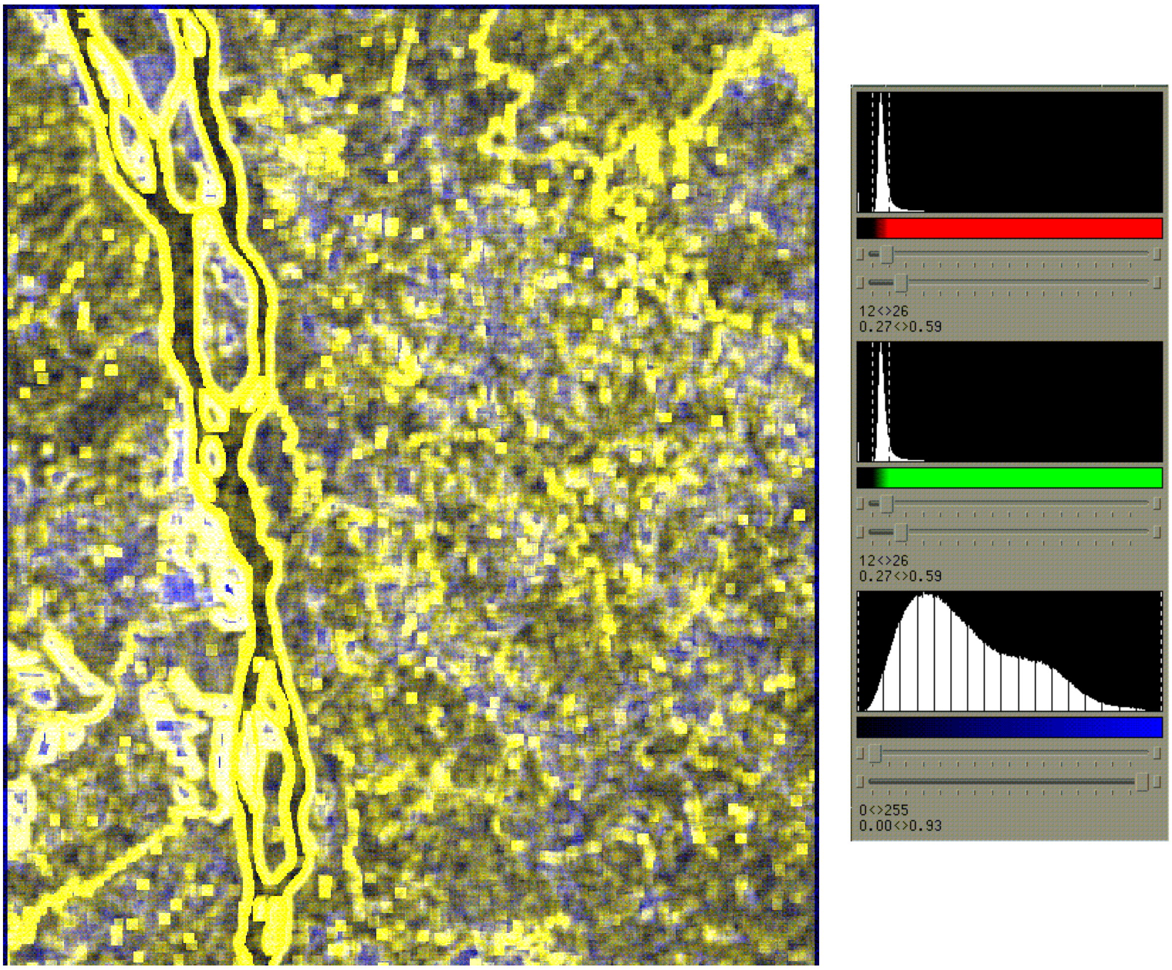

Figure 7 Overlay of Figure 4(d) (red and green) with Figure 1(c) (blue).